

Neutron Scattering Study of the Low-Frequency Vibrations in Vitreous Silica

U. Buchenau

Institut für Festkörperforschung, Kernforschungsanlage Jülich, D-5170 Jülich, West Germany

and

N. Nücker

Institut für Nukleare Festkörperphysik, Kernforschungszentrum Karlsruhe, D-7500 Karlsruhe, West Germany

and

A. J. Dianoux

Institut Laue-Langevin, F-38042 Grenoble Cedex, France

(Received 23 July 1984)

The vibrational excitations in vitreous silica above 150 GHz were investigated at 50, 100, and 290 K by inelastic scattering of cold neutrons. A detailed study of the frequency and wave-vector dependence shows that even at the lowest frequencies only a small part of the scattering is due to acoustic phonons. The type of motion of the dominating additional low-frequency modes is identified as a coupled rotation of SiO₄ tetrahedra. Possible connections to the low-temperature glass anomalies are discussed.

PACS numbers: 63.50.+x, 63.20.Dj, 65.40.Em

The nature of the low-frequency excitations in glasses is one of the major unsolved problems in solid state physics.¹⁻³ The unusual glass features are most clearly seen in vitreous silica. Its specific heat below 1 K is dominated by tunneling modes of unknown origin.^{1,2} The acoustic phonons show a linear dispersion up to 500 GHz (a frequency corresponding to a temperature of 25 K),⁴ but seem to be scattered at the high-frequency end of that region by strong unknown scattering centers.^{1,3} The specific heat between 2 and 10 K is enhanced by a factor two to three compared to the pure sound-wave contribution.^{1,5} In this Letter, we intend to show from inelastic neutron-scattering data that there are in fact not only acoustic phonons, but also other vibrational modes in this frequency range. The eigenvector of these modes will be analyzed from their inelastic structure factor.

The measurements were done with cold neutrons on the time-of-flight spectrometer IN6 at the Institut Laue-Langevin high-flux reactor at Grenoble. This spectrometer combines exceptionally high intensity with good energy resolution. The experimental difficulty is to measure accurately an inelastic intensity in the immediate neighborhood of an elastic line which is three orders of magnitude higher. We found a satisfactorily clean signal above neutron energy gains corresponding to a frequency of 150 GHz (nearly ten times the full resolution width away from the elastic line). Figure 1 shows data taken at 50, 100, and 290 K (normalized to 1 h measuring time, measured empty cryostat subtract-

ed, and corrected for a small tail of the elastic line which still persists up to 0.3 THz). The broad distribution at 290 K reproduces the earlier results of Leadbetter.⁶ At frequencies below 2 THz, the intensities scale essentially with the Bose factor. This shows that within the obtainable accuracy the 290-K data are representative for a temperature-independent density of vibrational states.

In the following we will analyze the character of these vibrational modes from their inelastic structure factor. We begin with the part that we know, namely the long-wavelength acoustic phonons. As

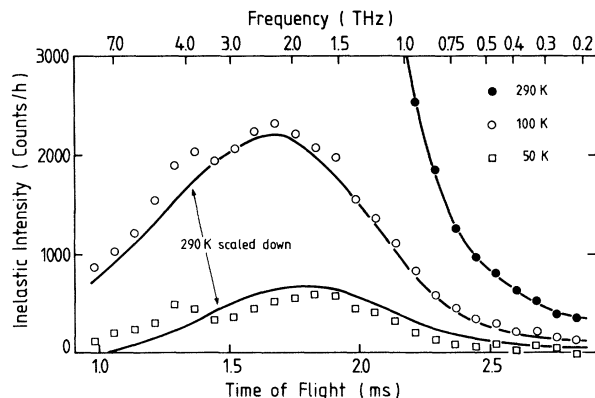


FIG. 1. Inelastic neutron-scattering intensities from vitreous silica at 50, 100, and 290 K. The data represent the sum of 19 detector groups between 60 and 114° scattering angle. The lines correspond to the 290-K data scaled down to 50 and 100 K by the adequate Bose factors.

was shown by Carpenter and Pelizzari,⁷ it is possible to calculate the inelastic scattering from sound waves in a glass without any adjustable parameter from the elastic scattering, the temperature, the density, and the sound velocities. We used simplified formulas from a recent reformulation of their work done by one of us⁸:

$$d\sigma^{(0)}/d\Omega = I_0(Q), \quad (1)$$

and

$$d\sigma^{(1)}/d\Omega d\omega = (k_f/k_i) (\hbar Q^2/2M_{av}) f_B(Z(\omega)/\omega) (1/2) \int_{-1}^{+1} dz I_0(Q + q_\omega z) \quad (2)$$

[$d\sigma^{(0)}/d\Omega$ is the elastic-scattering cross section (both for coherent and incoherent scattering), $d\sigma^{(1)}/d\Omega d\omega$ is the double-differential cross section for scattering by sound waves, $\vec{Q} = \vec{k}_i - \vec{k}_f$ is the scattering vector, M_{av} is the average atomic mass, f_B is the Bose factor, $Z(\omega)$ is the density of states]. q_ω is the average momentum vector of the sound waves at the frequency ω . In our frequency region it is so small that the inelastic structure factor for sound waves is practically given by $Q^2 I_0(Q)$. The sound-wave density of states can be calculated from

$$Z(\omega) = V_{av}/(2\pi^2\bar{c}^3) \quad (3)$$

(V_{av} average atomic volume, \bar{c}^3 directional average over the sound velocities).

The integrated elastic intensity $I_0(Q)$ obtained in the IN6 is shown in Fig. 2. The measurement was extended to higher momentum transfer values by a subsequent measurement on the triple-axis spectrometer SV4 at the reactor DIDO in Jülich. The inelastic intensity calculated from this $I_0(Q)$ and an average sound velocity¹ of 4.1 km/s is shown in Fig. 3 for a frequency of 0.7 THz, together with measured data. It is obvious that the sound-wave

scattering explains only a small part of the observed intensity. There is a Q independent part which we assign to multiple scattering because it is present at small Q where the intensity should be practically zero. But there is also a steep rise toward higher Q which can be attributed neither to sound waves nor to multiple scattering.

In order to analyze this strong additional scattering, we subtracted the calculated sound-wave scattering from the measured 290-K data in the whole frequency region from 0.15 to 2.5 THz. It turns out that the remaining intensities exhibit a frequency-independent structure factor. This is shown in Fig. 4, where the intensities at different frequencies have been plotted together after proper scaling. The maximum at 1.5 \AA^{-1} which is characteristic for sound waves in this material and which in fact also appears in the data before subtraction (see Fig. 3) is no longer visible in Fig. 4. There is a steep rise above 2.3 \AA^{-1} and a pronounced shoulder at 2.85 \AA^{-1} . Clearly, this scattering is not due to sound waves.

Which vibrational mode may be expected to have a low frequency in vitreous silica apart from the sound waves? We can guess the answer to this

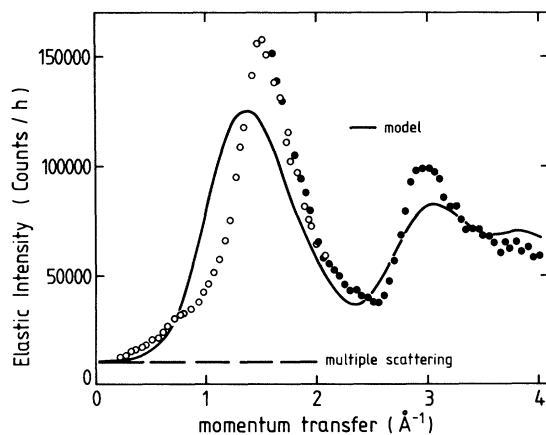


FIG. 2. Elastic scattering from vitreous silica at 290 K: open circles, integrated elastic line from IN6; solid circles, properly scaled data measured on the triple-axis SV4 in the elastic setting.

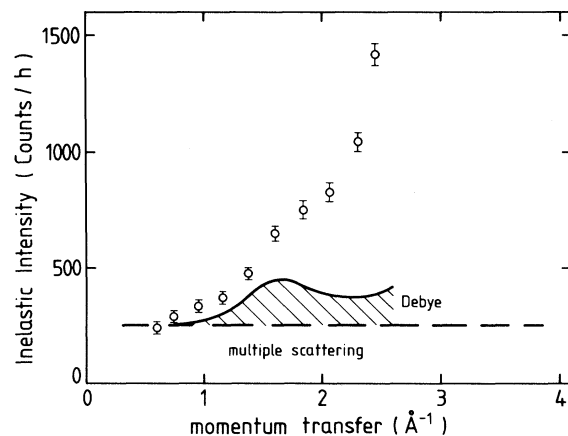


FIG. 3. Inelastic scattering from vitreous silica at 290 K between 0.6 and 0.8 THz. The shaded area corresponds to the scattering from sound waves.

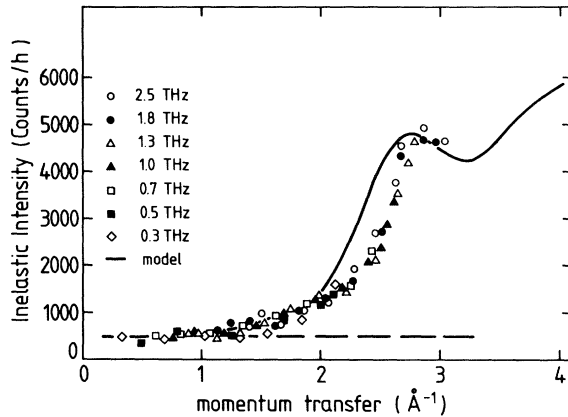


FIG. 4. Inelastic structure factor of vitreous silica at 290 K after subtraction of the sound-wave scattering for different frequencies. Intensities scaled to the intensity at 1.0 THz.

question both from the different polymorphic crystalline forms⁹ occurring for SiO_2 and from measured phonon dispersion curves of quartz.¹⁰⁻¹³ We expect vitreous silica to be built from SiO_4 tetrahedra sharing each of their corners with one other tetrahedron in a continuous three-dimensional network. Though the corner linkage between tetrahedra cannot be considered as a freely movable hinge, it is certainly the softest spring in the system.¹⁴ Therefore it is natural to assume coupled rotations of neighboring SiO_4 tetrahedra as the soft modes in vitreous silica.

In order to check whether the measured inelastic structure corresponds to coupled rotations of neighboring SiO_4 tetrahedra, the elastic and inelastic scattering intensities were calculated by use of a simple model (Fig. 5). A central SiO_4 tetrahedron is connected to four outer tetrahedra. The elastic scattering from a glass consisting of such units was calculated in the spirit of the quasicrystalline model.¹⁵ Naturally, the model is so crude that it only reproduces the essential features of the elastic scattering, but in this work we are not trying to find out fine details about the atomic positions; we are doing a rough analysis of the atomic motion. For simplification, we assumed stretched Si-O-Si bonds (structural investigations¹⁶ give an average Si-O-Si angle of 153°). The resulting deviations from the elastic scattering were partially compensated by the assumption of a shorter Si-O distance (1.54 Å instead of 1.6 Å). As seen from Fig. 2, the elastic intensities are reasonably well reproduced.

The inelastic structure factor was calculated⁷ for the pattern of coupled rotations shown in Fig. 5. We note that the three possible rotations of the

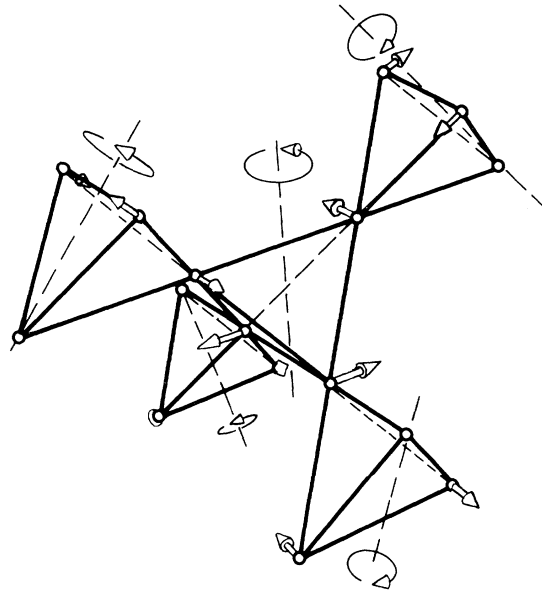


FIG. 5. Model of coupled rotations of the SiO_4 tetrahedra in vitreous silica.

central tetrahedron in our model are degenerate, so that all three give the same inelastic structure factor. After appropriate scaling, one gets the continuous line in Fig. 4, which corresponds rather closely to the measured data. An assumed rotation of only the central tetrahedron gives a broad intensity maximum at 3 \AA^{-1} which fails to reproduce the measurements. Thus, while we are not able to tell how far these modes extend from the central tetrahedron into the glass, they certainly involve a coupled rotation of the nearest neighbors.

We can use the model to determine the density

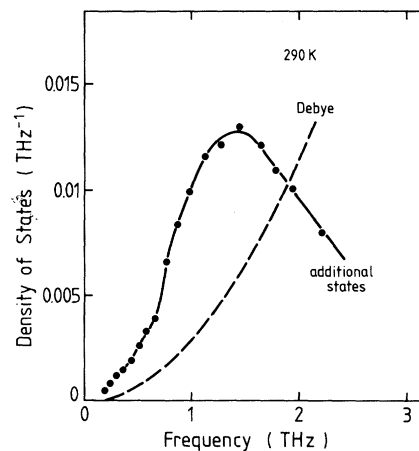


FIG. 6. Density of states of additional modes in vitreous silica compared to the Debye density of states.

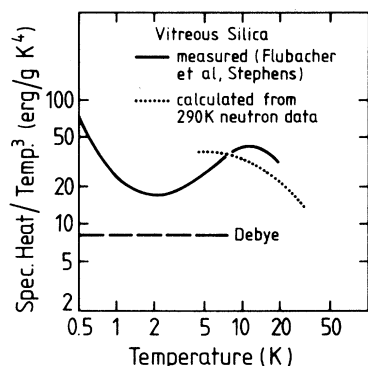


FIG. 7. Comparison of the heat capacity calculated from the neutron results at 290 K to measured data.

of these vibrational states on an absolute scale via the normalization of the elastic scattering to the measured one. The density of states thus obtained is shown in Fig. 6. One can use these results to calculate the specific heat. Figure 7 shows a comparison of the specific heat calculated in this way to measured data.^{1,5} Though the agreement is far from perfect, it seems obvious that neutron scattering and specific heat see the same vibrational states in this frequency, or equivalently, temperature, region. The peak at about 12 K in the low-temperature heat-capacity data seems to shift toward lower temperatures in the data calculated from the room-temperature neutron scattering.

The modes observed here explain one of the low-temperature glass anomalies in vitreous silica, namely the excess heat capacity between 1 and 10 K which gives rise to the anomalous T^3 term in the specific heat. We have not studied the detailed connection to the other low-temperature anomalies. There are, however, strong arguments that such a connection does indeed exist. There will be a resonant interaction between these low-frequency vibrations and the acoustic phonons¹⁷ which could explain the strong scattering^{1,3} of the acoustic phonons above 200 GHz. Furthermore, the existence of a low-frequency vibrational mode implies a soft potential in its configurational coordinate. The specific shape of this soft potential will vary at random according to the specific surroundings at a given place in the glass. It is likely that in some cases two (or more) minimum configurations of the SiO_4 tetrahedra exist which are separated by a small

energy barrier. In such cases the soft potential becomes a double minimum potential. The tunneling centers are then those configurations where the difference in the minimum energies corresponds to temperatures below 1 K. The number 10^{17} cm^{-3} of the tunneling states seems to be compatible with the $3 \times 10^{21} \text{ cm}^{-3}$ vibrational states that we see. This picture corresponds to one of the possible models discussed by Anderson, Halperin, and Varma.¹⁸

Stimulating discussions with H. Grimm, S. Hunklinger, and H. R. Schober are gratefully acknowledged.

¹R. B. Stephens, Phys. Rev. B **13**, 852 (1976).

²S. Hunklinger and W. Arnold, in *Physical Acoustics*, edited by W. P. Mason and R. N. Thurston (Academic, New York, 1976), Vol. 12, p. 155.

³M. P. Zaitlin and A. C. Anderson, Phys. Rev. B **12**, 4475 (1975).

⁴M. Rothenfusser, W. Dietsche, and H. Kinder, Phys. Rev. B **27**, 5196 (1983).

⁵P. Flubacher, A. J. Leadbetter, J. A. Morrison, and B. P. Stoicheff, J. Phys. Chem. Solids **12**, 53 (1959).

⁶A. J. Leadbetter, J. Chem. Phys. **51**, 779 (1969).

⁷J. M. Carpenter and C. A. Pelizzari, Phys. Rev. B **12**, 2391 (1975).

⁸U. Buchenau, unpublished.

⁹H. D. Megaw, in *Crystal Structures: A Working Approach* (Saunders, Philadelphia, 1973), pp. 259–269.

¹⁰M. M. Elcombe, Proc. Phys. Soc., London **91**, 947 (1967).

¹¹J. D. Axe and G. Shirane, Phys. Rev. B **1**, 342 (1970).

¹²H. Grimm and B. Dorner, J. Phys. Chem. Solids **36**, 407 (1975).

¹³B. Dorner, H. Grimm, and H. Rzany, J. Phys. C **13**, 6607 (1980).

¹⁴T. H. K. Barron, C. C. Huang, and A. Pasternak, J. Phys. C **9**, 3925 (1976).

¹⁵A. J. Leadbetter and A. C. Wright, J. Non-Cryst. Solids **7**, 23 (1972).

¹⁶E. H. Henninger, R. C. Buschert, and LeRoy Heaton, J. Phys. Chem. Solids **28**, 423 (1967).

¹⁷A. A. Maradudin, E. W. Montroll, G. H. Weiss, and I. P. Ipatova, *Theory of Lattice Dynamics in the Harmonic Approximation, Solid State Physics: Advances in Research and Applications* (Academic, New York, 1971).

¹⁸P. W. Anderson, B. I. Halperin, and C. M. Varma, Philos. Mag. **25**, 1 (1972).